JGV Papers in Press. Published November 7, 2014 as doi:10.1099/vir.0.070870-0

ROLE OF THE LIPID RAFTS IN THE LIFE CYCLE OF CANINE CORONAVIRUS

Annamaria Pratelli*, Valeriana Colao

Department of Veterinary Medicine – University of Bari - Italy

*Department of Veterinary Medicine
Strada per Casamassima Km 3
70010 Valenzano – Bari
Italy
Tel: +39 080 4679835
Fax: +39 080 4679843
email: annamaria.pratelli@uniba.it

Main Text Word Count: 3540
Summary Word Count: 250
Number of Figures: 8

Running title: Canine coronavirus infectivity and cholesterol

Summary

Coronaviruses are enveloped RNA viruses that have evolved complex relationship with their host cells and modulate their lipid composition, lipid synthesis and signaling of host cell. Lipid rafts, enriched in sphingolipids, cholesterol and associated proteins, are special plasma membrane microdomains involved in several processes of viruses infections. The extraction of cholesterol leads to disorganization of lipid microdomains and to dissociation of proteins bound to the lipid rafts. Because of cholesterol-rich microdomains appear to be a general feature of the entry mechanism of nonenveloped viruses and of several coronaviruses, the purpose of this study was to analyze the contribution of lipids in the infectivity of canine coronavirus (CCoV). CCoV lifecycle is closely connected to plasma membrane cholesterol, from cell entry to viral particle production. The methyl-β-cyclodextrin (MβCD) was employed to remove cholesterol and to disrupt the lipid rafts. Cholesterol depletion from cellular membrane resulted in a dose-dependent reduction but not in the abolishment of virus infectivity and at a concentration of 15 mM, the reduction of the infection rate was about 68%. MβCD treatment to verify if cholesterol in the envelope was required for CCoV infection, resulted in a dose-dependent inhibitory effect and at a concentration of 9 mM MβCD infectivity was reduced by about 73%. Since viral entry would constitute a target for antiviral strategies, inhibitory molecules interacting with viral and/or cellular membranes or interfering with the function of lipid metabolism, could offer strong antiviral potential. It will be interesting in future to analyze the membrane microdomains in CCoV envelope.

INTRODUCTION

Coronaviruses (CoVs), a genus in the *Coronaviridae* family, are large, enveloped, positive-sense RNA viruses, 27.6 to 31 kb in length, responsible for highly prevalent diseases in humans, birds and domestic animals. The one-third in the 3'end of the genome contains ORFs encoding for the major structural proteins, spike (S), envelope (E), membrane (M), hemoagglutinin-esterase (HE) and nucleocapsid (N) proteins. These ORFs are interspersed with several ORFs encoding for different non-structural proteins, most of which of unknown function (Lai & Holmes, 2001; Pratelli, 2006, 2011). In rooted trees, the members of the coronavirus genus consistently form three distinct monophyletic groups, referred to as phylogroups 1, 2 and 3. Canine coronaviruses (CCoVs) are included in phylogroup 1. In view of the recent increase in the number of newly-discovered coronaviruses and ensuing debates and confusion in the literature concerning coronavirus taxonomy, the unofficial, but widely accepted, nomenclature has been proposed to the ICTV Executive Committee, and phylogroups 1 through 3 were converted into genera designated *Alpha-*,

Beta- and *Gammacoronavirus*, respectively (Pratelli, 2011). *Deltacoronavirus* is a new genus proposed in July 2013 (ictvonline.org/virustaxonomy) (Table 1).

Lipid rafts are special plasma membrane microdomains with an increased structural order, designated liquid ordered domains in model membranes. Lipid rafts, enriched in sphingolipids, cholesterol and associated proteins, play a critical role in different biological aspects of the life cycle of several viruses and are involved in many processes of viruses infection. In particular, the tight packaging of the sphingolipids is maintained by the presence of cholesterol, a major constituent of the lipid rafts, and several proteins partition into these membrane domains (Imhoff *et al.*, 2007). Extraction of cholesterol destroys this order, leading both to the disorganization of the lipid rafts microdomains and to the dissociation of proteins bound to the lipid rafts (Barman & Nayak, 2007).

The role of cholesterol in the entry of nonenveloped viruses was demonstrated for Simian Virus 40 (SV40), rotavirus, rhinovirus and enterovirus (Anderson *et al*., 1996; Suzuki & Suzuki, 2006). Successful virus entry of enveloped viruses requires the binding to specific cellular receptors and the fusion of the viral membrane with the cellular membrane. Accumulating evidences suggest that enveloped virus entry may require cholesterol in either of the two membranes involved, or in both. Human Immunodeficiency Virus (HIV) type-1 infection requires cholesterol both in the target cell membrane and in the viral envelope (Guyader *et al*., 2002; Liao *et al.*, 2001, 2003). Cholesterol in both membranes is also required for Bovine Herpesvirus 1 (BoHV-1) infection of MDBK cells (Zhu *et al*., 2010). For other viruses in the *Alphaherpesvirinae* subfamily of the *Herpesviridae*, such as Herpes Simplex Virus 1 (HSV-1), Varicella-Zoster Virus (VZV) and Porcine Pseudorabies Virus (PRV), cell membrane cholesterol is required during virus entry (Bender *et al*., 2003; Hambleton *et al*., 2007; Desplanques et al., 2008). Other viruses are sensitive to cholesterol depletion from the cellular membrane, such as Semliki Forest Virus (SFV), Murine Leukemia Virus (MLV), Ebola Virus (EBOV) and Marburg Virus Disease (MVD) (Ahn *et al.*, 2002; Bavari *et al*., 2002; Lu *et al.*, 2002; Phalen & Kielian, 1991). For influenza virus and Duck Hepatitis B Virus (DHBV) the presence of cholesterol in its viral envelope is critical, but it is not essential in the target cell (Sun & Whittaker, 2003; Funk *et al*., 2008), and recently it has been demonstrated that Canine Distemper Virus (CDV) also requires cholesterol in the viral envelope (Imhoff *et al*., 2007). In contrast, in the case of Vesicular Stomatitis Virus (VSV), replication is not affected by cholesterol depletion, and numerous strains of the *Flaviviridae* family, i.e. Dengue Virus (DENV) and Yellow Fever Virus (YFV), enter and infect cells independent of cholesterol (Umashankar *et al*., 2008).

It is known that coronaviruses differ in their tissue tropism and different cellular receptors are involved in virus entry. The depletion of cellular and viral cholesterol inhibits virus entry of

several coronaviruses: Mouse Hepatitis Virus (MHV) (Choi *et al*., 2005), Severe Acute Respiratory Syndrome (SARS)-CoV (Li *et al*., 2007), HCoV-229E (Nomura *et al*., 2004), TGEV (Ren *et al*., 2008) and avian Infectious Bronchitis Virus (IBV) (Imhoff *et al*., 2007). In the present study we investigated to our knowledge the role of cholesterol in the viral envelope and in the cellular membrane for CCoV infection of A72 cells. The methyl-β-cyclodextrin (MβCD), a cholesterol-binding agent, was employed to remove cholesterol and to disrupt the lipid rafts.

RESULTS

Infection efficiency after cholesterol depletion from cellular membrane

To investigate if cellular cholesterol was essential for CCoV entry into susceptible cells, A72 monolayers were mock pretreated or pretreated with various concentrations of MβCD and subsequently infected with CCoV strain SE/97. Cells were cultured and virus yield was determined with virus titration assay. MβCD treatment of A72 cells resulted in an abatement of the virus production in a dose-dependent manner, suggesting that cell membrane cholesterol is necessary at the virus entry stage for CCoV infection. At a concentration of 15 mM, the reduction of the infection rate was about 68% (Fig. 1a).

To confirm that the inhibitory effects for CCoV replication at the virus entry stage were due to cholesterol depletion, cell membrane cholesterol was replenished with different concentrations of exogenous cholesterol and the recovery of virus infection was analyzed. Cholesterol-depleted cells (pretreated with 15 mM MβCD) were incubated with exogenous cholesterol, infected with CCoV and virus yield was investigated with virus titration assay. As shown in Fig. 1b the inhibitory effect was reversed with cholesterol replenishment and virus production was partially restored to values close to those observed prior to MβCD treatment. At a concentration of 700 μg ml^{-1}, infectivity was restored to an average of 77% compared to the mock treated cells.

The concentration of MβCD and cholesterol employed in this study did not cause significant adverse effect on cell viability (data not shown).

Infection efficiency after cholesterol depletion from viral membrane

To analyze whether cholesterol in the viral envelope is required for CCoV entry in susceptible cells, the virus was mock treated or treated with different concentrations of MβCD prior to infection. Cell monolayers were incubated with non-treated and MβCD-treated viral suspensions and virus yield was determined with virus titration assay. As reported in Fig. 2a, the exposure of CCoV to MβCD resulted in a dose-dependent inhibitory effect on the virus infectivity. In particular at a concentration of 9 mM MβCD, virus yield was reduced by about 73%.

To verify whether the effect of cholesterol depletion was reversible, exogenous cholesterol at various concentrations was added virus suspension pretreated with 9 mM MβCD. Cholesterol replenishment resulted in an increase of the infectivity of CCoV and at concentration of 700 μg ml^{-1} infectivity reached about 82% of the value observed prior to cholesterol depletion (Fig. 2b).

Cellular and viral cholesterol measurement

A72 cells were treated with various concentrations of MβCD and cellular cholesterol was determined with Amplex® Red Cholesterol Assay Kit. MβCD treatment resulted in a dose-dependent reduction of the cholesterol content in the lipid rafts microdomains of the A72 plasma membrane. In particular 15 mM of MβCD reduced the amount of cellular cholesterol of about 60% (Fig. 3a). A72 pretreated with 15 mM of MβCD were analyzed after cholesterol replenishment by addition of exogenous cholesterol in increasing amounts. As shown in Fig. 3b, 700 μg ml^{-1} of exogenous cholesterol restore the cholesterol values of the cellular membranes nearly to the values determined prior to MβCD treatment.

Amplex® Red Cholesterol Assay Kit was also employed to determine viral cholesterol. MβCD was used to deplete cholesterol and increasing drug concentrations resulted in a dose-dependent decrease of cholesterol content from viral membrane. At a concentration of 9 mM MβCD, viral cholesterol was reduced of about 70% (Fig. 3c). Cholesterol depleted virions were replenished with exogenous cholesterol in increasing amounts and virus pellets were used for cholesterol measurements. 700 μg ml^{-1} of exogenous cholesterol restored the cholesterol values of the viral membranes nearly to the values determined prior to MβCD treatment (Fig. 3d).

DISCUSSION

Viruses are intracellular parasites entirely dependent upon the host cell system for replication and spreading. In the case of enveloped viruses viral nucleocapsid is surrounded by a lipid membrane, derived from the infected cell, where glycoproteins are fixed supporting the functions of entry into target cells and/or fusion between viral and cellular membranes. The lipid composition of animal membranes is complex, and three main categories of lipids can be distinguished: glycerophospholipids, sphingolipids and sterols. Sphingolipids are main components of animal cell membranes, and sphingomyelin at the plasma membrane is known to be enriched in lipid microdomains forming the so-called “rafts” together with cholesterol (Blaising & Pécheur, 2013). These lipids contribute to viral infection by modulating the properties of viral and/or cellular membranes during infection and can thus play a role through their preferential partitioning into the membrane microdomains. Specifically, viral entry brings together virions and host cells that will

interact in a subtle-controlled step-by-step process: each step therefore relies on a paired combination of lipids and proteins (Blaising & Pécheur, 2013).

Viruses have evolved complex relationship with their host cells and many viruses modulate lipid composition, lipid synthesis and signaling of their host cell (Blasing & Pécheur, 2013). In particular, lipids are essential for the life cycle of several coronaviruses. The depletion of cellular cholesterol inhibits virus entry of MHV (Thorp & Gallagher, 2004; Choi *et al*., 2005), SARS-CoV (Li *et al.*, 2007; Glende *et al*., 2008), HCoV-229E (Nomura *et al*., 2004) and IBV (Thorp & Gallagher, 2004; Nomura *et al*., 2004; Li *et al*., 2007; Imhoff *et al*., 2007). Ren *et al*. (2008) showed the importance of cholesterol in both the cellular and viral membranes for TGEV infection and in addition a functional analysis suggested that cholesterol depletion affects a post-adsorption step in TGEV entry process (Yin *et al*., 2010). Therefore, the importance of cholesterol-rich microdomains appears to be a general feature of the entry mechanism of different viruses and, as far as coronaviruses are concerned, the purpose of this study was to analyze the contribution of lipids in the infectivity of CCoV, and in particular whether cholesterol was important as a constituent of the virus, of the host cells or of both. CCoV lifecycle appears to be closely connected to plasma membrane cholesterol. In the case of TGEV and HCoV-229E, the cholesterol dependence is consistent with the presence of porcine and human aminopeptidase N, respectively (Ren et al., 2008). Conversely, MHV and SARS-CoV use different receptors, MHVR and ACE2, respectively, which are nonraft-proteins (Thorp & Gallagher, 2004; Warner *et al*., 2005).Our analysis did not provide evidence that the activities of the S protein, binding to sialic acids and to aminopeptidase N, were reduced in cholesterol-depleted virions. However, optimal infectivity of CCoV requires cholesterol in plasma membrane. In particular, cholesterol depletion resulted in a reduction but not in the abolishment of virus infectivity and virus entry may occur also at lower cholesterol levels but increased cholesterol makes this process more efficient. At a concentration of 700 $\mu g\ ml^{-1}$, infectivity was restored to an average of 77% compared to the mock treated cells, confirming that the reduction was due to the cholesterol depletion, and that the inhibitory effects was partially reversible.

Interestingly, our study also demonstrated the role of cholesterol in the viral membrane. This datum is particularly important because coronaviruses mature by a budding process at the early compartments of the secretory pathway (Tooze *et al*., 1984), where the content of cholesterol and sphingolipids is lower compared to the plasma membrane (Sevlever *et al*., 1999). As observed for TGEV by Ren *et al*. (2008) our results confirmed the possibility that lipid microdomains exist in the membrane of CCoV, and the low concentration of cholesterol may explain why the infectivity of CCoV *in vitro* is affected by MβCD-concentrations lower than those that affect infectivity of other

viruses like HIV and influenza virus. It will be interesting in future studies to analyze the membrane microdomains in the CCoV envelope.

Lipids and receptors for lipids are therefore key players in the early stages of CCoV infection, i.e. entry and fusion. These stages are amenable to antiviral strategies, and molecules inhibiting CCoV entry and/or fusion could likely act on extracellular targets, thereby limiting virus-induced cell damages. By analogy, as observed for hepatitis C virus by Blaising & Pécheur (2013), molecules targeting lipids or their receptors could be considered as CCoV-entry inhibitors and the virus could be employed as animal model to test coronaviruses antiviral. Viral entry is a key target for antiviral strategies and molecules and/or drugs interacting with viral and/or cellular membranes or interfering with the function of lipid metabolism regulators, could be considered potential antiviral and could constitute potent therapeutics against coronavirus infection combined to already existing strategies.

Future work has to address the question whether cholesterol facilitates coronavirus entry by affecting the membrane fluidity or whether other molecular interactions depend on an increased content of cholesterol.

METHODS

Cell and virus

The A72 canine fibroma cell line, established from a tumour surgically removed from a female 8-year-old Golden Retriever dog (Binn *et al.*, 1980), was employed. The cells were maintained in Dulbecco Minimal Essential Medium (DMEM) supplemented with 5% foetal calf serum (FCS) and passaged twice a week. CCoV strain SE/97 ("SE" stands for "Seeing Eye Dogs", Pennsylvania isolate) was employed throughout the study. The virus, gently supplied from Prof. L.E. Carmichael (Cornell Vet, Ithaca – New York), was isolated on A72 cells from an adult dogs with mild enteritis and recovered within a week. SE/97 was propagated on A72 cells and grown in serum-free medium. The viral titre was determined in 96-well microtitration plates with A72 cells and was expressed as $TCID_{50}$ $50\mu l^{-1}$ calculated using the Reed-Muench formula (Reed & Muench, 1938). CCoV-induced cytophatic effect of infected cells was determined based on the appearance of enlarged, bizarrely shaped cells followed by focal cell detachment. The infectivity titre of the stock virus was $10^{5.5}$ $TCID_{50}$ $50\mu l^{-1}$.

Reagents

The methyl-β-cyclodextrin (MβCD) (C4555, Sigma-Aldrich) is a strictly surface-acting drug that can selectively and rapidly remove cholesterol from the plasma membrane in preference to other membrane lipids (Barman & Nayak, 2007). This cholesterol depletion reagent has been widely

employed in studying the effect of both cholesterol depletion and lipid raft disassembly, and current data indicate that it inhibits virus entry of several viruses (Choi *et al*., 2005; Li *et al*., 2007; Nomura *et al*., 2004; Imhoff *et al*., 2007; Ren *et al*., 2008). To remove the plasma membrane cholesterol, concentrations of 3, 6, 9, 10, 12, 15 mM of MβCD in DMEM were prepared.

Water soluble cholesterol (C4951, Sigma Aldrich) was employed to replenish cholesterol after extraction of cellular and viral cholesterol using MβCD.

Cholesterol depletion and replenishment from cellular membrane at the virus-entry stage

To remove cholesterol from cellular membrane, cells monolayers seeded in 24-well plates, containing approximately 300.000 A72 cells/per well, were washed three times with DMEM and incubated for 30 min at 37°C in a CO_2 incubator with serum-free DMEM in the absence (mock cells) or in the presence (treated cells) of MβCD at the concentrations of 3, 6, 9, 10, 12, 15 mM. To determine if cellular cholesterol depletion at the virus-entry stage affects virus replication, MβCD-treated or mock cells were washed three time with DMEM to remove MβCD and incubated with 100 $TCID_{50}$ $50\mu l^{-1}$ of virus suspension at 37°C for 1 h. Fresh DMEM was then applied and the cells were incubated for 48 h in a CO_2 incubator. For investigation of the infection efficiency, MβCD-treated or mock cells were frozen e thawed three time and subjected to virus titration in A72 cells as described above.

For cholesterol replenishment, monolayers of A72 cells in 24-well plates, containing approximately 300.000 A72 cells/per well, were mock pretreated or pretreated with 15 mM MβCD for 30 min at 37°C to remove cellular membrane cholesterol as described above. The concentrations of 15 mM was selected because in the cholesterol depletion test, it was the optimal MβCD concentration not producing collateral effects for A72 cells.

The cells were then washed three times with DMEM, replenished with different concentrations of water-soluble cholesterol in DMEM ranging from 400 to 800 $\mu g\ ml^{-1}$ and incubated for 1 h at 37°C. Mock cells were replenished with serum-free medium. For cell infection analysis after cellular cholesterol replenishment, the cells were washed three times with DMEM, and viral suspensions containing 100 $TCID_{50}$ $50\mu l^{-1}$ were applied to the cell monolayers. The plates were incubated for 1 h at 37°C (Zhu *et al*., 2010), fresh DMEM was applied and the cells were incubated for 48 h in a CO_2 incubator. For investigation of the infection efficiency, treated or mock cells were frozen e thawed three time and subjected to virus titration in A72 cells as described above.

The reduction and the restoration of viral infectivity were converted to percentages for an immediate understanding of the reduced and restored amounts, respectively.

All the experiments were repeated twice under the same conditions.

Cholesterol depletion from viral membrane and effect on virus infectivity

For viral cholesterol extraction, 1 ml of viral suspensions containing 100 $TCID_{50}$ $50\mu l^{-1}$ were incubated with MβCD at the concentrations of 3, 6, 9, 10, 12, mM, respectively for 1 h at 37°C. To determine if the virus cholesterol was essential for CCoV infectivity, after cholesterol depletion from viral membrane, cell monolayers were washed three times with DMEM and then incubated with MβCD-treated viral suspensions at 37°C for 1 h. To avoid negative effects of MβCD on A72 cells, the inoculums was diluted 1:3 in DMEM before infection. The controls were mock treated. Finally, treated cells and controls were washed three times with DMEM and incubated for 48 h in a CO_2 incubator. To analyze the infection efficiency after viral cholesterol depletion, the monolayers were frozen e thawed three time and subjected to virus titration in A72 cells as described above.

For cholesterol replenishment, 1 ml of CCoV suspensions were mock treated or treated with 9 mM MβCD for 30 min at 37°C, then replenished with different concentrations of water-soluble cholesterol in DMEM ranging from 400 to 800 $\mu g\ ml^{-1}$ and incubated for 1 h at 37°C. The concentrations of 9 mM was selected because in the cholesterol depletion test, it was the optimal MβCD concentration not producing collateral effects for CCoV. Mock cells were replenished with serum-free medium. For cell infection analysis after viral cholesterol replenishment, the cells were washed three times with DMEM, and cholesterol-replenished or non-replenished (control) viral suspensions were applied to the cell monolayers and incubated at 37°C for 48 h (Ren *et al*., 2008). For investigation of the infection efficiency, samples were frozen e thawed three time and subjected to virus titration in A72 cells as described above.

The reduction and the restoration of viral infectivity were converted to percentages for an immediate understanding of the reduced and restored amounts, respectively.

All the experiments were repeated twice under the same conditions.

Cellular and viral cholesterol content measurement

Cellular and viral cholesterol were measured using the Amplex® Red Cholesterol Assay Kit (A12216, Invitrogen/Life Technologies) according to manufactured instructions and according to protocols reported by Ren *et al*. (2008).

To determine cellular cholesterol, confluent monolayer of A72 cells grown on six-well plate were treated with different concentrations of MβCD ranging from 3 to 15 mM. At the same time, monolayers of A72 cells in six-well plate pretreated with 15 mM of MβCD, were replenished with various concentrations of exogenous cholesterol ranging from 400 to 800 $\mu g\ ml^{-1}$. All the monolayers were then washed three times with DMEM, trypsinised with EDTA, centrifuged at 800 x g at 4°C for 5 min to remove cellular debris and the pellets were suspended in PBS. The cellular cholesterol concentration was determined in triplicase with the Amplex® Red Cholesterol Assay Kit. Non-treated A72 cells were used as control.

To determine viral cholesterol, 1 ml of two different viral suspensions ($10^{5.5}$ $TCID_{50}$ μl^{-1} each) were treated in parallel with MβCD for cholesterol depletion, specifically one suspension with different concentrations of the drug from 3 to 12 mM and the other with 9 mM. Both suspensions were then treated with exogenous water-soluble cholesterol by applying final concentrations ranging from 400 to 800 $\mu g\ ml^{-1}$. The suspensions were centrifuged at 800 x g at 4°C for 5 min to remove cellular debris and then ultracentrifuged at 140.000 rpm for 1 h at +4°C. The pellets were suspended in PBS and subjected to cholesterol concentration determination in triplicase with the Amplex® Red Cholesterol Assay Kit. Non-treated virus was employed as control.

All the experiments were repeated twice under the same conditions.

It should be noted that CCoV was grown in serum-free medium to avoid that cholesterol measurement was affected by serum cholesterol.

ACKNOWLEDGEMENTS

The authors would like to thank their colleagues at the Department of Veterinary Medicine, Section Infectious Diseases at the University of Bari, Italy, whose collaboration has been essential to accomplish the present study.

REFERENCES

Ahn, A., Gibbons, D. L. & Kielian, M. (2002). The fusion peptide of Semliki Forest virus associates with sterol-rich membrane domains. *J Virol* **76**, 3267–3275.

Anderson, H. A., Chen, Y. & Norkin, L. C. (1996). Bound simian virus 40 translocates to caveolin-enriched membrane domains, and its entry is inhibited by drugs that selectively disrupt caveolae. *Mol Biol Cell* **7**, 1825–1834.

Barman, S. & Nayak, D. P. (2007). Lipid Raft Disruption by Cholesterol Depletion Enhances Influenza A Virus Budding from MDCK Cells. *J Virol* **81**, 12169–12178.

Bavari, S., Bosio, C. M., Wiegand, E., Ruthel, G., Will, A. B., Geisbert, T. W., Hevey, M., Schmaljohn, C., Schmaljohn, A. & Aman, M. J. (2002). Lipid raft microdomains: a gateway for compartmentalized trafficking of Ebola and Marburg viruses. *J Exp Med* **195**, 593–602.

Bender, F. C., Whitbeck J. C., Ponce de Leon M., Lou H., Eisenberg, R. J. & Cohen, G. H. (2003). Specific association of glycoprotein B with lipid rafts during herpes simplex virus entry. *J Virol* **77**, 9542–9552.

Binn, L. N., Marchwicki, R. H. & Stephenson, E. H. (1980). Establishment of a canine cell line: derivation, characterization, and viral spectrum. *Am J Vet Res* **41**, 855-860.

Blaising, J. & Pécheur, E. -I. (2013). Lipids-A key for hepatitis C virus entry and a potential target for antiviral strategies. *Biochimie* **95**, 96-102.

Choi, K. S., Aizaki, H. & Lai, M. M. (2005). Murine coronavirus requires lipid rafts for virus entry and cell–cell fusion but not for virus release. *J Virol* **79**, 9862–9871.

Desplanques, A. S., Nauwynck, H. J., Vercauteren, D., Geens, T. & Favoreel, H. W. (2008). Plasma membrane cholesterol is required for efficient pseudorabies virus entry. *Virology* **376**, 339–345.

Funk, A., Mhamdi, M., Hohenberg, H., Heeren, J., Reimer, R., Lambert, C., Prange, R. & Sirma, H. (2008). Duck hepatitis B virus requires cholesterol for endosomal escape during virus entry. *J Virol* **82**, 10532–10542.

Glende, J., Schwegmann-Wessels, C., Al-Falah, M., Pfefferle, S., Qu, X., Deng, H., Drosten, C., Naim, H. Y. & Herrler, G. (2008). Importance of cholesterol-rich membrane microdomains in the interaction of the S protein of SARS-coronavirus with the cellular receptor angiotensin-converting enzyme 2. *Virology* **381**, 215–221.

Guyader, M., Kiyokawa, E., Abrami, L., Turelli, P. & Trono, D. (2002). Role for human immunodeficiency virus type 1 membrane cholesterol in viral internalization. *J Virol* **76**, 10356–10364.

Hambleton, S., Steinberg, S. P., Gershon, M. D. & Gershon, A. A. (2007). Cholesterol dependence of varicella-zoster virion entry into target cells. *J Virol* **81**, 7548–7558.

Imhoff, H., von Messling, V., Herrler, G. & Haas, L. (2007). Canine distemper virus infection requires cholesterol in the viral envelope. *J Virol* **81**, 4158–4165.

Lai, M. M. C. & Holmes, K. V. (2001). Coronaviridae: the viruses and their replication. In *Fields Virology*, pp. 1163-1185. Edited by D. M. Knipe, P. M. Howley, D. E. Griffin, R. A. Lamb, M. A. Martin, B. Roizman & S. E. Strais. Philadelphia, Lippincott Williams & Wilkins.

Li, G. M., Li, Y. G., Yamate, M., Li, S. M. & Ikuta, K. (2007). Lipid rafts play an important role in the early stage of severe acute respiratory syndrome-coronavirus life cycle. *Microbes Infect* **9**, 96–102.

Liao, Z., Cimakasky, L. M., Hampton, R., Nguyen, D. H. & Hildreth, J. E. (2001). Lipid rafts and HIV pathogenesis: host membrane cholesterol is required for infection by HIV type 1. *AIDS Res Hum Retroviruses* **17**, 1009–1019.

Liao, Z., Graham, D. R. & Hildreth, J. E. (2003). Lipid rafts and HIV pathogenesis: virion-associated cholesterol is required for fusion and infection of susceptible cells. *AIDS Res Hum Retroviruses* **19**, 675–687.

Lu, X., Xiong, Y. & Silver, J. (2002). Asymmetric requirement for cholesterol in receptorbearing but not envelope-bearing membranes for fusion mediated by ecotropic murine leukemia virus. *J Virol* **76**, 6701–6709.

Nomura, R., Kiyota, A., Suzaki, E., Kataoka, K., Ohe, Y., Miyamoto, K., Senda, T. & Fujimoto, T. (2004). Human coronavirus 229E binds to CD13 in rafts and enters the cell through caveolae. *J Virol* **78**, 8701–8708.

Phalen, T. & Kielian, M. (1991). Cholesterol is required for infection by Semliki Forest virus. *J Cell Biol* **112**, 615–623.

Pratelli, A. (2006). Genetic evolution of canine coronavirus and recent advances in prophylaxis. *Vet Res* **37**, 191-200.

Pratelli, A. (2011). The evolutionary processes of canine coronaviruses. *Adv Virol* **2011**, 1-10.

Reed, L. J. & Muench, H. (1938). A simple method of estimating fifty percent endpoints. *Am J Hyg* **27**, 493–497.

Ren, X., Glende, J., Yin, J., Schwegmann-Wessels, C. & Herrler, G. (2008). Importance of cholesterol for infection of cells by transmissible gastroenteritis virus. *Virus Res* **137**, 220–224.

Sevlever, D., Pickett, S., Mann, K. J., Sambamurti, K., Medof, M. E. & Rosenberry, T. L. (1999). Glycosylphosphatidylinositol-anchor intermediates associate with triton-insoluble membranes in sub cellular compartments that include the endoplasmic reticulum. *Biochem J* **343**, 627–635.

Sun, X. & Whittaker, G. R. (2003). Role for influenza virus envelope cholesterol in virus entry and infection. *J. Virol.* **77**, 12543–12551.

Suzuki, T. & Suzuki, Y. (2006). Virus infection and lipid rafts. *Biol Pharm Bull* **29**, 1538–1541.

Thorp, E. B. & Gallagher, T. M. (2004). Requirements for CEACAMs and cholesterol during murine coronavirus cell entry. *J Virol* **78**, 2682–2692.

Tooze, J., Tooze, S. & Warren, G. (1984). Replication of coronavirus MHV-A59 in saccells: determination of the first site of budding of progeny virions. *Eur J Cell Biol* **33**, 281–293.

Umashankar, M., Sánchez-San Martín, C., Liao, M., Reilly, B., Guo, A., Taylor, G. & Kielian, M. (2008). Differential cholesterol binding by class II fusion proteins determines membrane fusion properties. *J Virol* **82**, 9245–9253.

Warner, F. J., Lew, R. A., Smith, A. I., Lambert, D. W., Hooper, N. M. & Turner, A.J. (2005). Angiotensin-converting enzyme 2 (ACE2), but notACE, is preferentially localized to the apical surface of polarized kidney cells. *J Biol Chem* **280**, 39353–39362.

Yin, J., Glende, J., Schwegmann-Wessels, C., Enjuanes, L., Herrler, G. & Ren, X. (2010). Cholesterol is important for a post-adsorption step in the entry process of transmissible gastroenteritis virus. *Antiviral Res* **88**, 311–316.

Zhu, L., Ding, X., Tao, J., Wang, J., Zhao, X. & Zhu, G. (2010). Critical role of cholesterol in bovine herpesvirus type 1 infection of MDBK cells. *Vet Microbiol* **144**, 51–57.

Table 1: *Coronaviridae* classification and important viruses in the *Alphacoronavirus* genus

Order	Family	Subfamily	Genus	Species
Nidovirales	*Coronaviridae*	*Coronavirinae*	*Alphacoronavirus*	*Human Coronaviruses 229E, NL63* *Trasmissible Gastroeneteritis Virus TGEV* *Porcine Respiratory Coronavirus PRCoV* *Porcine Epidemic diarrhea Virus PEDV* *Canine coronaviruses CCoVs* *Feline Coronaviruses FCoVs* Miniopterus bat coronaviruses Bat-CoV-1, HKU8 Rhinolophus bat coronavirus *Rh-Bat-CoV*-HKU2 Scotophilus bat coronavirus *Sc-Bat-CoV-512*
			Betacoronavirus *Deltacoronavirus* *Gammacoronavirus*	
		Torovirinae		
	Arteriviridae *Mesoniviridae* *Roniviridae*			

Figures legend

Fig. 1

CCoV infection efficiency after cholesterol depletion and replenishment from cellular membrane. **a**) MβCD treatment of A72 cells reduced infectivity of CCoV in a dose-dependent manner and at a concentration of 15 mM, viral titre suffered a reduction of about 68%. **b**) Cholesterol-depleted cells were replenished with exogenous cholesterol and virus production was partially restored.

The 100% infectivity value corresponds to the original titre of the stock virus.

Fig. 2

CCoV infection efficiency after cholesterol depletion and replenishment from viral membrane. **a**) MβCD treatment of CCoV reduced infectivity in a dose-dependent manner and at a concentration of 9 mM, viral titre suffered a reduction of about 73%. **b**) Replenishment of cholesterol in the viral membrane resulted in an increase of CCoV infectivity.

The 100% infectivity value corresponds to the original titre of the stock virus.

Fig. 3

Cholesterol content determination after depletion and replenishment of cholesterol from the cellular membrane (**a**, **b**) and from the viral membrane (**c**, **d**). Cholesterol content was determined with Amplex® Red Cholesterol Assay Kit. **a**) Cellular cholesterol depletion with various concentration of MβCD. **b**) Recovery of cellular cholesterol after exogenous cholesterol replenishment. **c**) Viral cholesterol depletion with various concentration of MβCD. **d**) Recovery of viral cholesterol after exogenous cholesterol replenishment.

Fig. 1a

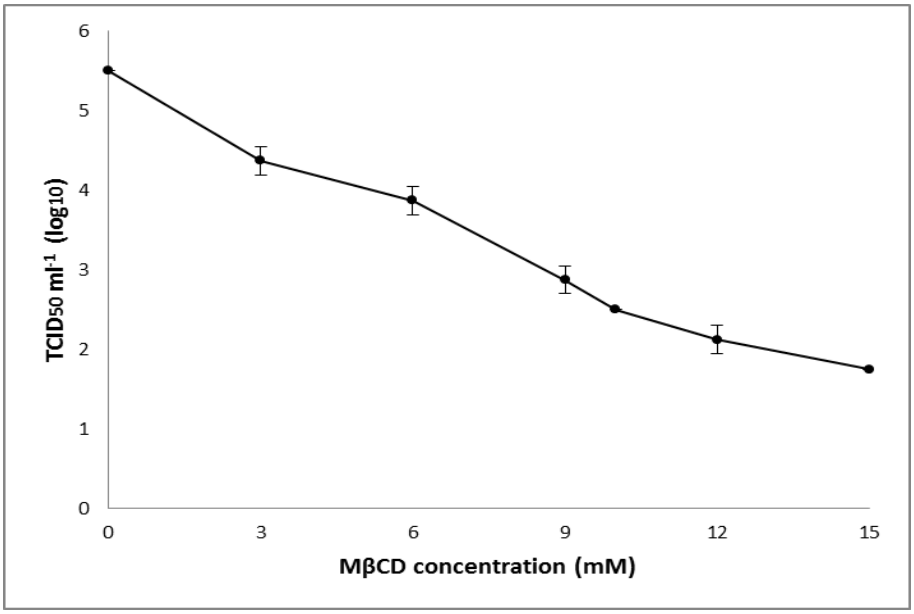
TCID50 ml-1 (log10)
0
1
2
3
4
5
6
0
3
6
9
12
15
MβCD concentration (mM)

Fig. 1b

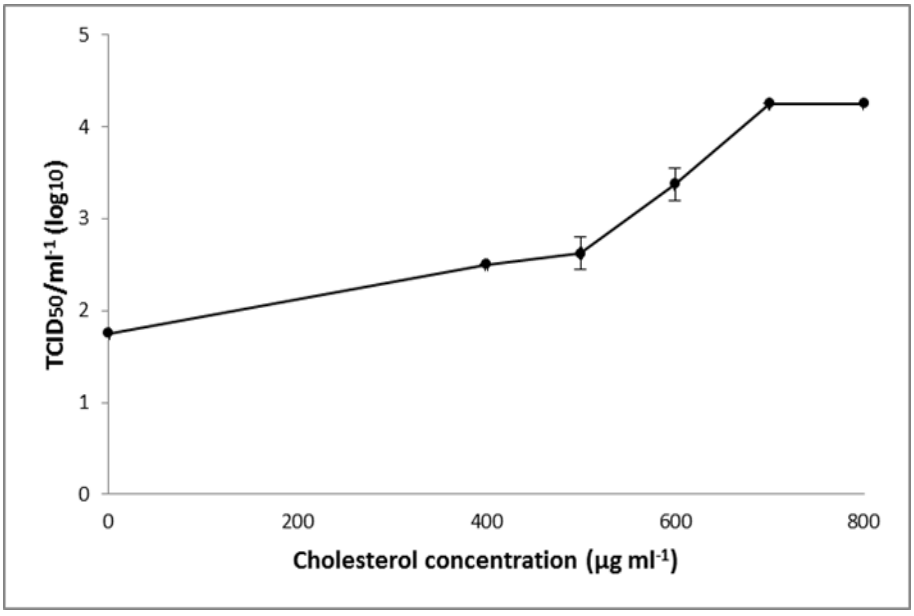
TCID50/ml-1 (log10)
0
1
2
3
4
5
0
200
400
600
800
Cholesterol concentration (µg ml-1)

Fig. 2a

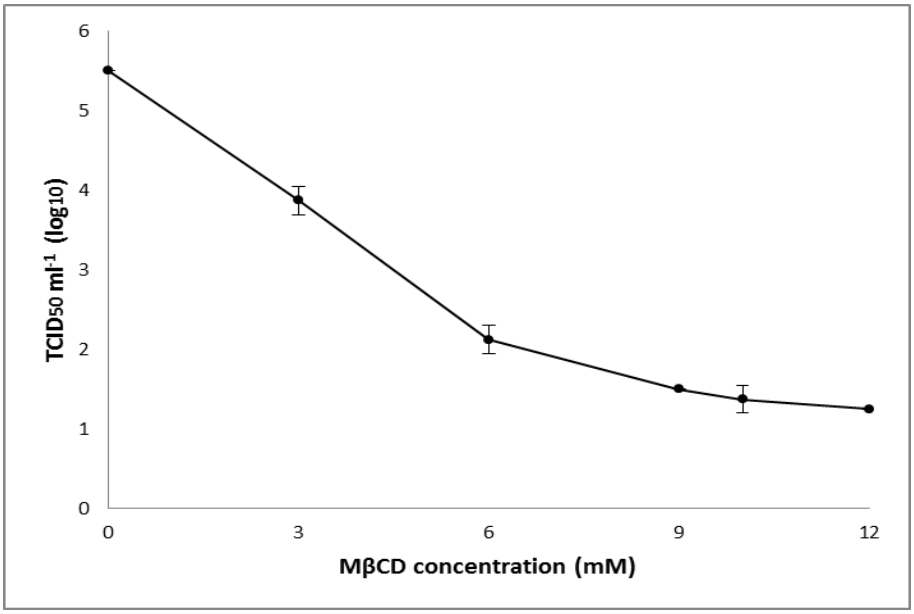
TCID50 ml-1 (log10)
0
1
2
3
4
5
6
0
3
6
9
12
MβCD concentration (mM)

Fig. 2b

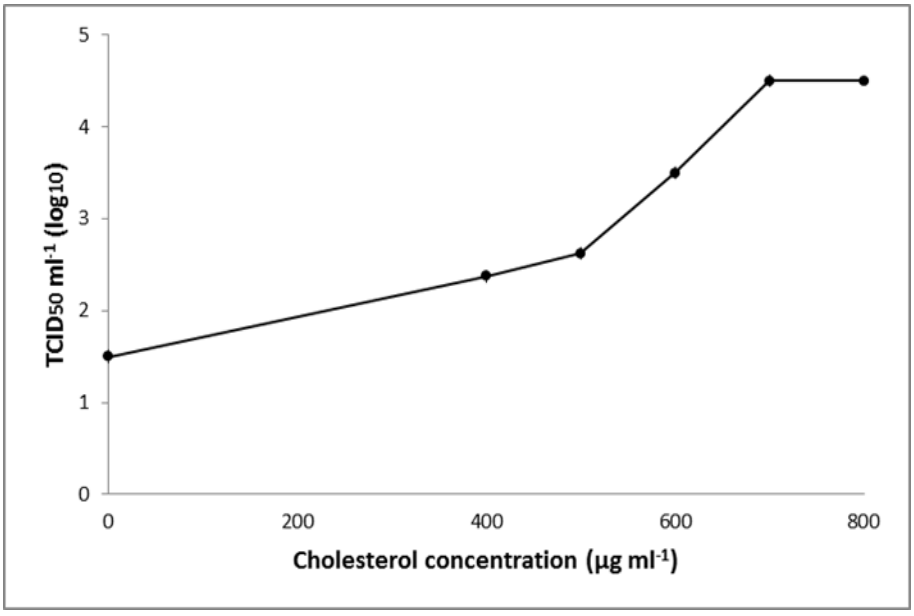
TCID50 ml-1 (log10)
0
1
2
3
4
5
0
200
400
600
800
Cholesterol concentration (µg ml-1)

Fig. 3a

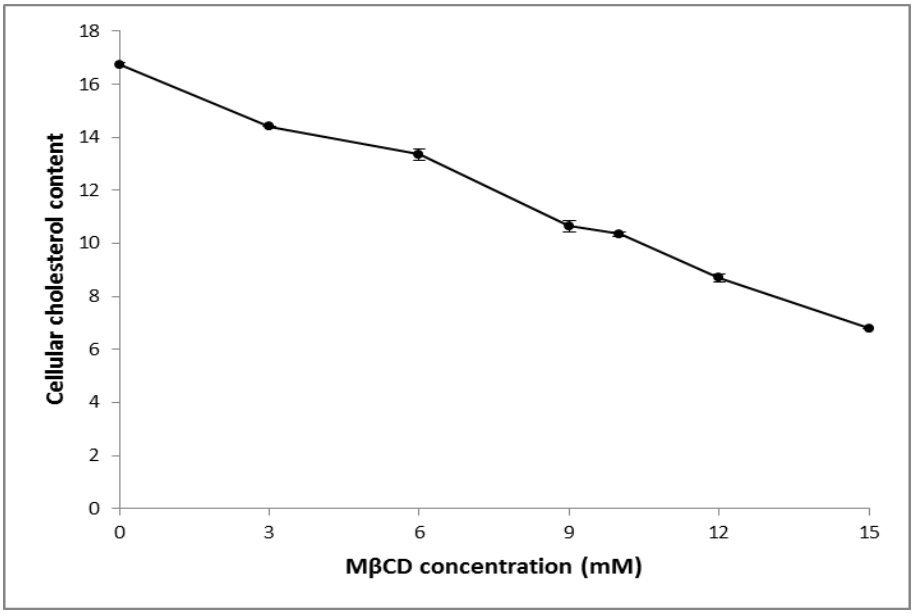
Cellular cholesterol content
18
16
14
12
10
8
6
4
2
0
0
3
6
9
12
15
MβCD concentration (mM)

Fig. 3b

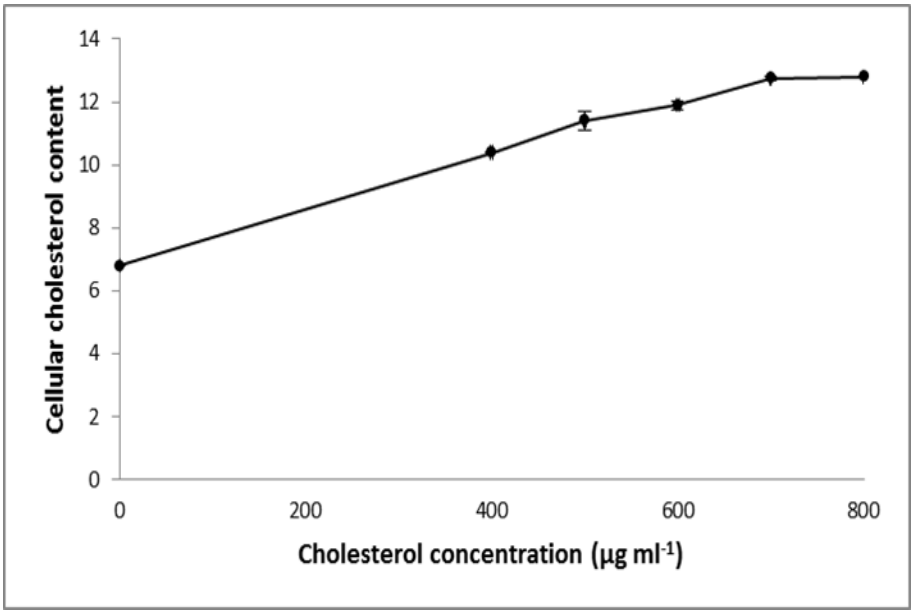
Cellular cholesterol content
14
12
10
8
6
4
2
0
0
200
400
600
800
Cholesterol concentration (µg ml-1)

Fig. 3c

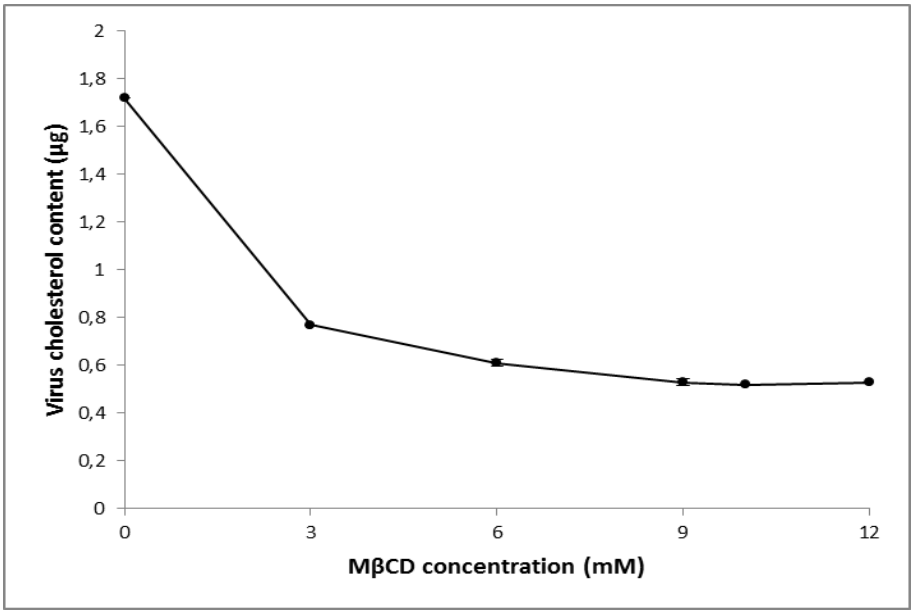
Virus cholesterol content (µg)
2
1,8
1,6
1,4
1,2
1
0,8
0,6
0,4
0,2
0
0
3
6
9
12
MβCD concentration (mM)

Fig. 3d

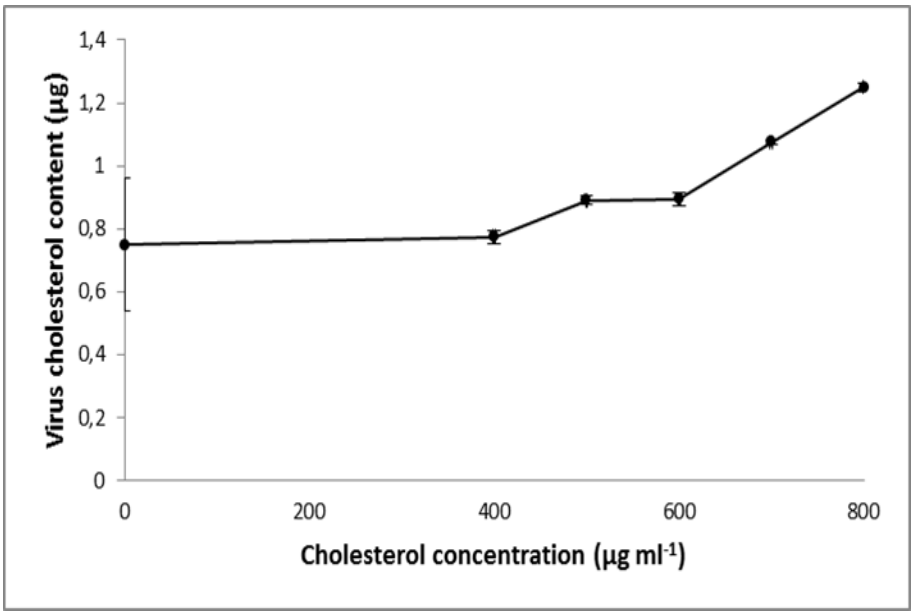
Virus cholesterol content (µg)
1,4
1,2
1
0,8
0,6
0,4
0,2
0
0
200
400
600
800
Cholesterol concentration (µg ml-1)